Plant, Cell & Environment

Plant, Cell and Environment (2012) **35**, 1601–1617 doi: 10.1111/j.1365-3040.2012.02512.x

Hydraulic limits preceding mortality in a piñon–juniper woodland under experimental drought

JENNIFER A. PLAUT[1], ENRICO A. YEPEZ[2], JUDSON HILL[1], ROBERT PANGLE[1], JOHN S. SPERRY[3], WILLIAM T. POCKMAN[1] & NATE G. MCDOWELL[4]

[1]*Department of Biology, MSC03 2020, 1 University of New Mexico, Albuquerque, NM 87131-0001, USA,* [2]*Departamento de Ciencias del Agua y del Medio Ambiente, Instituto Tecnológico de Sonora, Ciudad Obregón Sonora, 85000, Mexico,* [3]*Department of Biology, University of Utah, 257 South 1400 East, Salt Lake City, UT 84112, USA and* [4]*Earth and Environmental Sciences Division, Los Alamos National Laboratory, Los Alamos, NM 87545, USA*

ABSTRACT

Drought-related tree mortality occurs globally and may increase in the future, but we lack sufficient mechanistic understanding to accurately predict it. Here we present the first field assessment of the physiological mechanisms leading to mortality in an ecosystem-scale rainfall manipulation of a piñon–juniper (*Pinus edulis–Juniperus monosperma*) woodland. We measured transpiration (*E*) and modelled the transpiration rate initiating hydraulic failure (E_{crit}). We predicted that isohydric piñon would experience mortality after prolonged periods of severely limited gas exchange as required to avoid hydraulic failure; anisohydric juniper would also avoid hydraulic failure, but sustain gas exchange due to its greater cavitation resistance. After 1 year of treatment, 67% of droughted mature piñon died with concomitant infestation by bark beetles (*Ips confusus*) and bluestain fungus (*Ophiostoma* spp.); no mortality occurred in juniper or in control piñon. As predicted, both species avoided hydraulic failure, but safety margins from E_{crit} were much smaller in piñon, especially droughted piñon, which also experienced chronically low hydraulic conductance. The defining characteristic of trees that died was a 7 month period of near-zero gas exchange, versus 2 months for surviving piñon. Hydraulic limits to gas exchange, not hydraulic failure *per se*, promoted drought-related mortality in piñon pine.

Key-words: climate change; die-off; drought experiment; piñon; Sperry model; stomata.

INTRODUCTION

Drought-related tree mortality is a global phenomenon with significant implications for ecosystem structure and function (Bonal *et al*. 2008; Fensham, Fairfax & Ward 2009; Horner *et al*. 2009; Allen *et al*. 2010). Hypotheses that, alone or in combination, explain drought-related mortality in the absence of physical disturbances include catastrophic hydraulic failure, carbon starvation, and biotic factors such as insect and fungal pathogens (Suarez, Ghermandi & Kitzberger 2004; McDowell *et al*. 2008; Worrall *et al*. 2008; Adams *et al*. 2009; Brodribb & Cochard 2009). The role of each of these factors, and interactions among them, in the mechanism of mortality is expected to vary depending on future patterns of drought duration and intensity (Bigler *et al*. 2007; McDowell *et al*. 2008). It is not yet clear how mortality and its underlying mechanisms will respond to the anticipated increase in the frequency of extreme drought events with continued fossil fuel emissions (IPCC 2007; Fensham *et al*. 2009). Although drought-related mortality is a complex phenomenon, its accurate prediction is critical to modelling ecosystem responses and feedbacks to global climate change (Friedlingstein *et al*. 2006; Sitch *et al*. 2008).

Hydraulic failure is the complete loss of water transport to the canopy resulting from xylem embolism, the blockage of xylem conducting elements by air pulled across a pit membrane from an air-filled to a water-filled conduit (Tyree & Sperry 1988). Hydraulic failure can also occur in the rhizosphere when soil water potential (Ψ_s; see Table 1 for a list of symbols) declines below the air entry pressure, breaking the root–soil hydraulic connection (Sperry *et al*. 1998). This occurs during drought because Ψ_s decreases dramatically with proximity to the surface of an absorbing root as transpiration (E) continues. In both the xylem and the soil, hydraulic failure is linked to the decrease in water potential caused by flow at a given hydraulic conductance, and the associated decrease in hydraulic conductance that feeds back on water potential. The hydraulic limit to water transport is therefore defined as the critical transpiration rate (E_{crit}) which, under steady state conditions, generates a critical minimum xylem or soil water potential (Ψ_{crit}) that results in hydraulic failure (Sperry *et al*. 1998, 2002). Drought-related loss of conductance along the soil–plant continuum is a well-documented phenomenon (Sparks & Black 1999; Brodribb & Holbrook 2003; Brodribb & Cochard 2009; Iovi, Kolovou & Kyparissis 2009), but the frequency of hydraulic failure in field settings (i.e. non-potted plants), and whether it leads directly to mortality, is not well understood (Galvez & Tyree 2009; Resco *et al*. 2009; McDowell 2011).

Correspondence: J. Plaut. Fax: +1 505 277 0304; e-mail: jplaut@unm.edu

Table 1. List of symbols

Symbol		Units
E	Transpiration	
E_s	Sapwood-specific transpiration	mol m^{-2} s^{-1} expressed on a sapwood area basis
E_{pred}	Sapwood-specific transpiration predicted by the hydraulic model	mol m^{-2} s^{-1} expressed on a sapwood area basis
E_{crit}	Critical transpiration rate which, if allowed to reach steady state, would result in hydraulic failure somewhere in the soil-plant-atmosphere continuum	mol m^{-2} s^{-1} expressed on a sapwood area basis
J_s	Sap flux density	g m^{-2} s^{-1}
K	Soil-to-canopy hydraulic conductance	mol m^{-2} s^{-1} MPa^{-1}
K_{pred}	Soil-to-canopy conductance predicted by the hydraulic model at Ψ_{md} for a $\Delta\Psi$ of 0.2 MPa	mol m^{-2} s^{-1} MPa^{-1}
Ψ_l	Leaf water potential	MPa
Ψ_{pd}	Pre-dawn leaf water potential	MPa
$\Psi_{pd\text{-}pred}$	Pre-dawn leaf water potential predicted by the hydraulic model using K_{pred} and interpolated Ψ_{md}	MPa
Ψ_{md}	Midday leaf water potential	MPa
Ψ_{crit}	Critical leaf water potential which would result in hydraulic failure somewhere in the soil-plant-atmosphere continuum	MPa
$\Delta\Psi$	Difference between pre-dawn and midday water potential	MPa
Ψ_s	Soil water potential	MPa
ΔT	Difference between heated and unheated sap flow probes, corrected for the ambient axial temperature difference	°C
ΔT_{max}	Maximum daily temperature difference between heated and unheated sap flow probes, representing conditions of zero flow	°C

Plants reduce stomatal conductance in a manner consistent with regulating transpiration to avoid hydraulic failure (Sperry *et al*. 1998; Hacke *et al*. 2000; Cochard *et al*. 2002). Plant control of stomatal conductance and leaf water potential (Ψ_l) can be described by two broad strategies: isohydry and anisohydry (Tardieu & Simonneau 1998). Isohydric plants regulate Ψ_l above a minimum set-point; when drought pushes Ψ_s below this Ψ_l set-point, gas exchange ceases until precipitation increases Ψ_s. This stomatal response may minimize hydraulic failure, but it comes at the cost of limiting carbon assimilation and may predispose plants to carbon starvation, depending on the duration of the drought (McDowell *et al*. 2008; Breshears *et al*. 2009). Species with vulnerable xylem cannot experience a broad Ψ_l range without complete cavitation, and so would be expected to be relatively isohydric. Anisohydric plants allow Ψ_l to decrease with Ψ_s, allowing continued gas exchange during drought. Compared with isohydric species, anisohydric species maintain carbon assimilation at higher rates and further into drought, but the anisohydric strategy requires more cavitation-resistant xylem or else risks hydraulic failure under severe drought (McDowell *et al*. 2008). We note that there is not always a clear distinction between these two strategies, and that even typically anisohydric plants must constrain stomatal conductance at some point to avoid hydraulic failure (McDowell *et al*. 2008; Plaut *et al*., unpublished manuscript).

Piñon–juniper woodland [here *Pinus edulis* Engelm. and *Juniperus monosperma* (Engelm.) Sarg.] is a model system in which to study the hydraulic contributions to mortality during drought. Compared with juniper, piñon is more vulnerable to drought-induced xylem cavitation (Linton, Sperry & Williams 1998), is generally isohydric in its regulation of Ψ_l while juniper is generally anisohydric (Linton *et al*. 1998; West *et al*. 2008), and has recently exhibited greater mortality during drought (McDowell *et al*. 2008; Breshears *et al*. 2009; Floyd *et al*. 2009). Piñon also experiences episodic attacks by bark beetle, *Ips confusus* (LeConte), a vector for *Ophiostoma* fungi; juniper does not seem to have a pest with similar symbionts or outbreak cycles (Floyd *et al*. 2009). Previous analysis of hydraulic strategies in piñon and juniper has demonstrated that piñon spends a greater amount of time with near-zero gas exchange than juniper, but juniper experiences greater cavitation than piñon (West *et al*. 2007a, 2008). The mechanisms distinguishing mortality and survival during drought have not been previously experimentally tested.

Our study was designed to explicitly investigate hydraulic mechanisms underlying mortality in the field, using an ecosystem scale precipitation reduction mimicking the deficit that resulted in widespread mortality in 2002–2003 (precipitation ~50% below ambient). After less than 1 year, 67% of mature piñon (basal diameter > 9 cm, excluding a 5 m buffer zone from the edge of the drought treatment; 25% of piñon if all size classes and trees up to the plot edge are included) were attacked by bark beetles, infected with bluestain fungus, and died, giving us the opportunity to examine for the first time the physiology of field-grown trees leading up to mortality in a manipulative experiment. Our primary objective was to test the hypothesis that piñon's avoidance of hydraulic failure is associated with drought-related mortality through severe constraints on gas exchange, while juniper can sustain gas exchange

without hydraulic failure because of its greater resistance to cavitation.

METHODS

Site description

The study was conducted in the Los Piños mountains within the Sevilleta National Wildlife Refuge, Socorro County, New Mexico (N 34°23′13″, W 106°31′29″), part of the US Long-Term Ecological Research network. The elevation at the site is approximately 1911 m, which is close to the lower-elevation limit of piñon. Piñon and juniper are the dominant woody species; shrub live oak (*Quercus turbinella* Greene) is the only other woody species of any stature at the site (Table 2). Soils were calcid aridisols characterized as Sedillo-Clovis association of fan alluvium derived from conglomerate (Soil Survey Staff, Natural Resources Conservation Service, United States Department of Agriculture; http://websoilsurvey.nrcs.usda.gov/ accessed 28 February 2011). Long-term mean monthly temperatures range from 2.6 °C in January to 23.1 °C in July; annual precipitation averages 362 mm at a meteorological station near the site (Cerro Montoso meteorological station, 2.2 km from and approximately 70 m higher than the study site, 1989–2009, http://sev.lternet.edu/). Roughly half of the annual precipitation falls from convective storms during the North American Monsoon, typically during July through September.

The data for this study were acquired from a subset of plots in a larger precipitation manipulation experiment (Pangle *et al*., 2012). The four treatments applied were: (1) water addition; (2) water removal ('drought'); (3) cover control; and (4) ambient control. The larger experiment consisted of three blocks of the four treatments applied to 40 m × 40 m plots, established in the summer of 2007. We used study plots in a southeast-facing block of 8–18 degrees slope for the intensive physiology measurements to test our hypotheses. The water addition plots (#1 above) were not active during the period of this study and thus are not included in this paper.

The drought plot consists of UV-resistant clear acrylic sheets (Makrolon® SL, Sheffield Plastics, Sheffield, MA, USA) bent into troughs and screwed to rails approximately 1 m high. The sheets are 0.91 m wide and cover 0.81 m when bent. Troughs were inserted as far as possible into tree crowns without damaging the canopies, dammed and connected to the trough on the far side of the canopy with flexible 7.6 cm diameter hoses. Troughs drain to gutters, which divert water to existing arroyos. The rows of troughs together cover 45% of the plot. The cover control plot consists of the same plastic bent in the same way, but installed in a concave orientation, which replicates the microenvironment under the water removal troughs without removing ambient precipitation (Pangle *et al*., 2012). Installation of plastic covers on drought and cover control plots was completed on 22 August 2007. The ambient control plot had no treatment infrastructure installed.

Environmental data

A micrometeorological station at the research site included a Campbell Scientific HMP45C air temperature and relative humidity sensor (Logan, UT, USA), Campbell Scientific CS105 barometric pressure sensor, tipping bucket rain gauge equipped with a snowfall adapter (Texas Electronics, Dallas, TX, USA), R.M. Young 05103 wind monitor (velocity and direction; Campbell Scientific), Decagon EC-20 soil volumetric water sensor installed at 5 cm (Decagon Devices Inc., Pullman, WA, USA), net radiometer (model NR-LITE, Kipp & Zonen, Delft, The Netherlands), and a LI190SB PPFD/quantum sensor (Li-Cor, Lincoln, NE, USA). Sensors were operated via a Campbell Scientific CR10X datalogger, and continuous data were summed (rain gauge) or averaged over 30 min intervals.

Within each plot, five trees of each species were chosen for physiological measurements. Target trees were centrally located within the plots and had stem(s) of at least 9 cm diameter. Additionally, five intercanopy areas per plot were instrumented to measure soil water potential.

Soil moisture measurements

Plant-available soil moisture was measured with thermocouple psychrometers (Wescor Inc., Logan, UT, USA) controlled via Campbell Scientific CR-7 dataloggers. Soil psychrometer profiles were placed under each target tree and at the five designated intercanopy areas for a total of 15 profiles per plot. Each profile consisted of sensors at: (1) 15 cm; (2) 20 cm; and (3) as deep as could be augered and installed horizontally into the side wall of the hole, generally between 50 and 100 cm. Sensors were calibrated with four NaCl solutions of known water potential prior to field deployment.

Thermocouple psychrometers are accurate in their calibrated range but have range limitations in dry soils. Our sensors returned out-of-range values below soil water potentials of –6.5 to –7.5 MPa, typically during the

Table 2. Stand structure data

Species	Individuals per ha	Basal area, m^2 ha^{-1}	Crown area, m^2 ha^{-1}	Height, m
Piñon	140.6 ± 38.7	4.3 ± 1.0	1170 ± 159	2.8 ± 0.2
Juniper	296.9 ± 43.0	28.2 ± 3.7	2635 ± 185.6	2.7 ± 0.1

Data presented are means and standard errors based on measurements in four 1600 m^2 plots.

extended dry periods prior to the monsoons in 2007 and 2008, though some sensors continued to give valid output down to –8 MPa. Sensors that were observed to go out of range during those periods were assigned an endpoint of –8 MPa at the first major monsoonal storm of each season and a linear interpolation was constructed between their last reasonable point and that endpoint. This method avoids artificially raising the calculated mean as the driest sensors drop out of the array. This method is conservative because the general shape of a dry-down trajectory is exponential (van Genuchten 1980); therefore, approximating it with a linear function is more likely to overestimate than to underestimate water potential. The effect of this overestimation is likely to be minimal given that there is little plant-available water in the range of water potentials over which interpolation was conducted. Following soil re-wetting, sensors regained function, so drought period failure did not affect sample size over the long term.

Plant water potentials

Pre-dawn and midday leaf water potentials (Ψ_{pd} and Ψ_{md}, respectively) were measured throughout the study on each target tree using south-facing twigs with healthy foliage. Measurements were made monthly or with greater frequency when soil moisture was changing rapidly during each summer's dry-down and monsoon. Immediately following excision, samples were placed in a zip-top plastic bag with a small piece of damp paper towel (Kaufmann & Thor 1982; Kolb *et al*. 1998; Stone, Kolb & Covington 1999) and stored in a cooler until measurement with a Scholander-type pressure chamber (PMS Instruments, Corvallis, OR, USA). Midday samples were collected 10 at a time and measured sequentially to minimize the time since cutting, which was less than 1 h.

Sap flow measurements

Transpiration, E, was estimated by measuring sap flux density with Granier heat dissipation probes (Granier 1987; Phillips & Oren 2001). Two probes were installed on each target tree at least 1 m from the ground (path length) at a point where tree diameter was ≥9 cm. Probes were constructed at the University of New Mexico and installed during fall 2006 and early spring 2007. Each probe consisted of four 10 mm needles inserted radially into the xylem, 10 cm apart vertically and 5 cm apart horizontally. Each needle had an internal thermocouple 5 mm from the tip. One downstream needle was wrapped with 1 ohm cm^{-1} Advance resistance wire (Pelican Wire, Naples, FL, USA) and an aluminum sleeve was placed in the xylem prior to needle insertion to homogenize the heat input. The heated needle was supplied with 0.067 W, while the reference thermocouple in the unheated needle above it completed the standard Granier configuration. This amount of power is within the range used in other studies (Goulden & Field 1994; Bush *et al*. 2010), though on the low end to reduce power consumption and the risk of sapwood damage. The pair of reference thermocouples horizontally adjacent corrected for ambient axial thermal gradients (Goulden & Field 1994), an addition we found necessary due to the open canopy structure of this ecosystem and the resulting exposure of shielded probe locations and adjacent stems to direct solar radiation. This reference thermocouple set was added to existing sap flow sensors during spring 2007, but the response to the correction was not universal (i.e. it could not be applied retroactively, data not shown); only corrected data are reported here.

Temperature differentials (ΔT) during the daytime are corrected for T differences at zero flow (ΔT_{max}; Granier 1987) to calculate sap flux density, J_s. ΔT_{max} is generally assumed to occur at times unlikely to generate sap flux, that is, nights with low vapour pressure deficit (VPD), which are rare in this system. Applying each night's ΔT_{max} to the following day's temperature differentials removes the possibility of observing night-time sap flow, which can be a significant portion of daily water loss (Snyder, Richards & Donovan 2003). Further, ΔT_{max} was observed to drift over time in some instances, though changes were not correlated with night-time VPD. ΔT_{max} was also observed to shift periodically, sometimes randomly and at other instances when, for example, a probe was replaced. Therefore, we visually divided the time series of data into intervals of similar environmental characteristics and ΔT_{max} behaviour (i.e. direction of change) for each probe. Linear regressions of ΔT_{max} against time were generated for each interval and ΔT_{max} was set for each probe per day based on the value from the previous night, calculated from the regression. ΔT_{max} values, and J_s were calculated for each probe individually. This method may underestimate J_s because it does not guarantee that ΔT_{max} is calculated at zero flow conditions, but it does allow estimation of night-time flow while accounting for long-term change in ΔT_{max}.

Trees were cored near each sap flow probe during summer 2009 to assess the validity of the assumption that the 10 mm probes were located entirely within sapwood. Corrections were applied to sensors found to be measuring <10 mm sapwood (Clearwater *et al*. 1999). This correction was necessary for 4 out of the 10 juniper probes on each of the cover control and ambient control plots. No correction was necessary for any probes in piñon. For most of the juniper and all of the piñon, sapwood depth was greater than the length of the probe measuring sap flux density; therefore, we did not capture all of the variability in sap flux density. Sap flux density generally declines with distance from the cambium (Cohen *et al*. 2008), so we assume that we did capture the highest rates, but the scale of the project precluded installing probes at multiple depths. Based on site-specific equations (data not shown), we estimate that on average we sampled the outer 44% of sapwood area in piñon. In juniper, sapwood depth is so variable that while in most cases the probes were completely in sapwood, the average sapwood depth was less than the probe length. We used sap flux density as an indicator of plant functional status and did not scale to whole-tree water use (i.e. did not multiply measured sap flux densities by total sapwood

area). For all results presented, we converted J_s, g m^{-2} s^{-1}, to E_s, mol m^{-2} s^{-1} and did not scale to leaf area due to potentially changing leaf area, particularly as a function of treatment, during the course of the experiment. We also used the empirically derived coefficients in the Granier equation, which may have resulted in underestimation of sap flux density, though errors due to a lack of a species-specific calibration are generally more egregious for ring-porous than diffuse-porous or tracheid-bearing species (Bush *et al*. 2010).

Cavitation vulnerability

Curves describing xylem vulnerability to drought-induced cavitation (Sperry, Donnelly & Tyree 1988) were generated using the centrifuge technique (Cochard 2002; Cochard *et al*. 2005), adopting the conductivity calculation and protocol proposed by Li *et al*. (2008). Branch and root segments were cut as long as possible in the field, wrapped in a damp paper towel in a large plastic bag, placed in a cooler and transported 1 h to the lab. Samples were stored in a refrigerator in the lab and measured on the centrifuge within 24 h. Upon measurement, samples were cut under water to produce a straight segment with no branching or bark scarring approximately 25.5 cm long. Segment ends were trimmed with a new razor blade. Xylem pressure was generated with a Sorvall Model RC5C centrifuge (Thermo Fisher Scientific, Waltham, MA, USA) with custom rotors and conductance was measured using a 20 mM KCl solution filtered to 0.2 μm. Percent loss of conductance (PLC) was plotted against pressure and fit with a Weibull function to generate a vulnerability curve (Neufeld *et al*. 1992):

$$\mathrm{PLC} = 100\left(1 - e^{-\left(-\frac{\Psi}{b}\right)^c}\right) \quad (1)$$

Xylem vulnerability was measured on five piñon branches (trimmed lengths 254–258 mm, diameter without bark 5.7–7.3 mm), harvested in April and October 2008, and four piñon roots (trimmed lengths 251–255 mm, diameter without bark 6.5–10.0 mm), harvested in October 2008. Additionally, two juniper branches and two roots were measured, but due to the small sample size, the hydraulic model was parameterized with published vulnerability curves for this species (Willson, Manos & Jackson 2008). The vulnerability curves developed for juniper at our site showed them to be more vulnerable to cavitation than the published values used for modelling [xylem pressure at which 50% of conductance is lost, P_{50}, was –8.25 MPa for on-site juniper branches compared with –11.6 MPa reported by Willson *et al*. (2008)]. P_{50} for piñon branches was –2.75 MPa and P_{50} for piñon roots was –3.26 MPa, though the Weibull curve for the roots was steeper so that roots would achieve 100% cavitation earlier than branches. The Weibull function parameters for piñon branches were: $b = 3.43$ and $c = 1.65$, and for roots, $b = 3.57$ and $c = 4.07$.

Hydraulic model

Plant hydraulic limits were assessed using Sperry *et al*.'s (1998) model of water transport. The model solves the steady state of

$$E = K(\Psi_s - \Psi_l) \quad (2)$$

where K, mol m^{-2} s^{-1} MPa^{-1}, is the Ψ-dependent conductance of the entire soil-canopy pathway. The K is expressed on the same area basis as E (sapwood area, in our study). The modelled K depends on the seasonal maximum conductance and the 'b' and 'c' parameters of the Weibull function vulnerability curves. The model increments E and solves for Ψ_l to arrive at the maximum possible E (E_{crit}) and lowest Ψ_l (Ψ_{crit}) for a set of Ψ_s and vulnerability curve inputs. E greater than E_{crit} or Ψ_l lower than Ψ_{crit} would, theoretically, result in hydraulic failure somewhere along the transport pathway. At the same time, the model predicts E (E_{pred}) from measurements or estimates of Ψ_l. As we did not measure Ψ_{md} every day, linear interpolation between known points was used to generate a continuous Ψ_l record. Although it may be inaccurate when, for example, Ψ_{md} measurements bracket a large rain event, linear interpolation produced more reasonable estimates than linear models of Ψ_l based on physical parameters (data not shown).

Soil hydraulic conductivities were parameterized from soil texture data (Campbell 1985). Weibull parameters from the measured vulnerability curves were input separately for roots and canopy xylem to account for their differences in vulnerability to cavitation (Table 3). The E_s value used for each day's model input was the average of the 2 h period bracketing the daytime maximum E_s. Days with temperatures never above 0 °C and/or when maximum photosynthetically active radiation (PAR) was below 70% of the 9 d running maximum were excluded.

The model also requires the ratio of root:leaf area (A_r:A_l), which was not measured. Modelled E_{crit} saturates at high A_r:A_l as the xylem becomes more limiting than the rhizosphere. We chose A_r:$A_l = 3$ because it was sufficient to saturate E_{crit} in piñon, and to come within 5% of saturation averaged across the physiological range of Ψ_{pd} (approximately –1 to –8 MPa) in juniper.

Modelling scenario

In principle, the model can divide the rooting zone into three layers and use the measured soil water potentials as input. In practice, however, the data suggested that both species, though much more so for piñon, were drawing water from a missing soil layer that was wetter than any of the three measured layers. According to these data, on several days Ψ_{pd} and Ψ_{md} were less-negative than the wettest measured soil layer (a difference of several MPa in the case of piñon), and there was also significant soil water uptake as indicated by non-zero E_s. Furthermore, when Ψ_{md} is less-negative than the Ψ_s input for the model, the model cannot generate predictions of E_s, E_{crit} or Ψ_l because there is no driving gradient for flow from the soil to the canopy.

Table 3. Model input parameters

Parameter	Ambient piñon	Ambient juniper	Drought piñon	Drought juniper
Soil geometric mean particle size, mm	0.032	0.032	0.032	0.032
Geometric standard deviation of particle size	4.63	4.63	4.63	4.63
Soil bulk density	1.27	1.27	1.27	1.27
Silt fraction	0.4	0.4	0.4	0.4
Clay fraction	0.06	0.06	0.06	0.06
*Air entry potential, Ψ_e, MPa	–2.52	–2.52	–2.52	–2.52
*k_s, mol s^{-1} MPa^{-1} m^{-1} (saturated soil conductivity)	40.75	40.75	40.75	40.75
*b (soil texture parameter)	6.52	6.52	6.52	6.52
Branch Weibull b parameter	3.43	12.52	3.43	12.52
Branch Weibull c parameter	1.65	3.48	1.65	3.48
Root Weibull b	3.56	10.05	3.56	10.05
Root Weibull c	4.07	4.19	4.07	4.19
E_s at saturated k_l	0.69–2.65	0.9	0.8–1.2	0.6–0.8
*Saturated k_l, mol s^{-1} m^{-2} MPa^{-1}	0.6–2.3	1.04	0.92–1.38	0.69–0.92
LAI	1	1	1	1
A_r:A_l	3	3	3	3
r^2 of E_s:E_{pred}	0.99	0.998	0.87	0.995

Items preceded by an asterisk are calculated by the model but used as inputs. $\Psi_e = -0.5(GMD)^{-0.5}$ (Campbell 1985).

In the absence of the full soil moisture profile, the model was calibrated to predict Ψ_{pd} from the measured sap flow and Ψ_{md}:

$$\Psi_{pd\text{-}pred} = \frac{E_s}{K_{pred}} + \Psi_{md} \quad (3)$$

where K_{pred} is the soil-to-canopy hydraulic conductance at the Ψ_{md} calculated by the model for an arbitrarily small $\Psi_{pd} - \Psi_{md} = \Delta\Psi$ of 0.2 MPa. The calibration was run for the subset of days (between 1 April and 31 October) on which Ψ_{pd} was measured (7–9 d each year). The mean square error (MSE) between the $\Psi_{pd\text{-}pred}$ and the measured Ψ_{pd} was minimized by varying the initial K (K_{sat}) at the beginning of the time series. In piñon during 2007, the monsoon season corresponded with an obvious systematic deviation where $\Psi_{pd\text{-}pred}$ became much more positive than the measured Ψ_{pd}, indicating that K_{pred} was under-predicted post-monsoon (data not shown). This suggested recovery of hydraulic conductance in piñon, consistent with previous findings (West *et al*. 2008). In these cases, the model was calibrated separately for pre-monsoon and post-monsoon data. The model was also calibrated separately for 2007 and 2008 (April–October data only) to account for any changes in tree K occurring in the November to March period that was not modelled.

Once the model was calibrated, it was used to generate the full time sequence of K_{pred} and $\Psi_{pd\text{-}pred}$. The $\Psi_{pd\text{-}pred}$ time sequence was then input as Ψ_s for the entire rooting zone (in lieu of accurate profiles for Ψ_s and rooting depth). From the sequence of Ψ_s and interpolated Ψ_{md}, the model calculated E_{pred} and E_{crit}. Modelled K_{pred} was converted to PLC relative to the maximum K_{sat} per species obtained from the model calibration across both years and treatments. Because the ambient and cover control plots proved broadly similar in terms of Ψ_s, piñon and juniper E_s, and Ψ_l (see below), we applied the model only to ambient control and drought treatments. This method of using $\Psi_{pd\text{-}pred}$ as an integrated measure of the spatially heterogenous Ψ_s profile has been successful previously (West *et al*. 2008), though most of the previous applications of this model to isohydric *Pinus* species have been under relatively moist conditions (Ewers, Oren & Sperry 2000; Hacke *et al*. 2000; Domec *et al*. 2010).

Bark beetle activity

I. confusus (bark beetle) was identified in the field from pitch tubes on the main bole and larger branches and excavated galleries under the bark of affected piñon. *I. confusus* was subsequently identified in the lab based on Chansler (1964) and Wood (1982) and verified against existing reference collections at Rocky Mountain Research Station (Flagstaff, AZ, USA) and the Northern Arizona University Entomology laboratory (Flagstaff, AZ, USA).

Statistical analyses

Treatment effects on Ψ_s, Ψ_l and E_s were evaluated by comparing pretreatment with post-treatment differences. All pre- and post-treatment differences are provided in Supporting Information Table S1. Welch's *t*-tests were used to compare treatment differences in post-treatment periods with pretreatment differences. Wilcox signed-rank tests, which do not assume normal data distribution, were also used to compare daily E_s within species among plots. Because of the large number of tests performed, results were adjusted for a family-wise error rate of 5%. Effects of the rainfall manipulation treatments were considered significant if the post-treatment plot differences varied significantly from pretreatment differences (Supporting Information Table S1). Matlab® version 2007a (The

Mathworks, Natick, MA, USA) was used for all data management. R software (R Development Core Team 2008) was used for all statistical analysis.

RESULTS

In 2007 and 2008, mean daily temperature ranged from –8 °C to 30 °C (Fig. 1a) with an absolute range of –14.4 to 36.4 °C. VPD ranged from 0.02 to 5.5 kPa (Fig. 1b). Annual precipitation in 2007 and 2008 was 666 and 331 mm, respectively, compared with the 20 year average of 362 mm. The spring moisture pulse in 2008 was significantly smaller than that in 2007, and there were no precipitation events larger than 10 mm before July of that year (Fig. 1c). Between treatment imposition in late August 2007 and indications of piñon mortality in early August 2008, the site received 365 mm of precipitation, with the drought plot receiving an estimated 201 mm (55% of ambient, Fig. 5c). Needle browning on droughted piñon was observed in early August 2008, after ~11 months of treatment (Supporting Information Fig. S1). Onset of needle browning coincided with evidence of attack by *I. confusus*, and dying trees were also infected with *Ophiostoma* fungi (Porras-Alfaro, personal communication). Total piñon mortality on the drought plot reached 25% by December 2008 (6 out of 24 piñon within the plot boundary), though 67% of candidate target trees (basal diameter ≥9 cm and inside the 5 m plot buffer) died by that point and 100% by the following spring, with zero

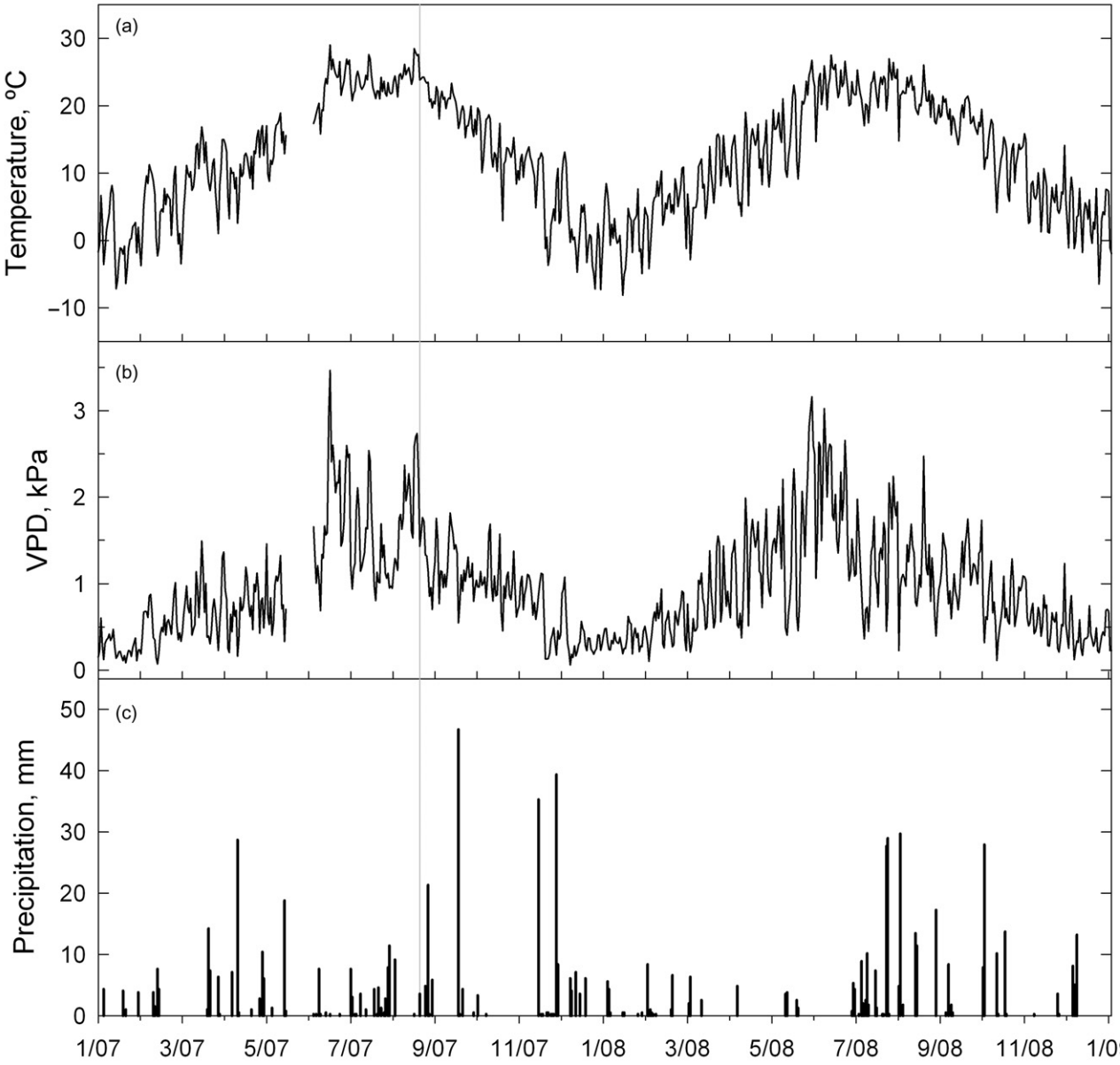

Figure 1. Climate data over the study period showing (a) mean daily temperature, (b) mean daily vapour pressure deficit (VPD) and (c) precipitation events. Vertical lines indicate initiation of treatments.

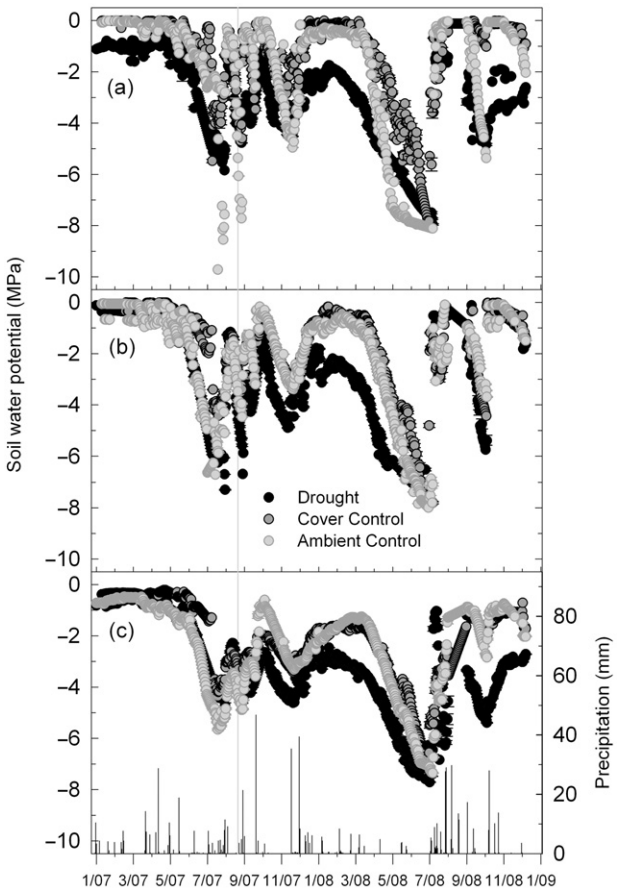

Figure 2. Soil water potential at (a) 15 cm, (b) 20 cm and (c) 50–100 cm for the drought (black), cover control (dark grey) and ambient control (light grey) treatments. Symbols are the mean of 15 sensors ± standard error, weighted by cover type (piñon, juniper, intercanopy). Vertical lines indicate initiation of treatments.

mortality of either species on the ambient and cover control plots.

Soil and plant water potentials

Rainout structures produced significant differences in Ψ_s compared with plots receiving ambient rainfall (Supporting Information Table S1, Fig. 2). Treatment effects became apparent almost immediately after treatment installation (Fig. 1c). The drought plot, which was drier than the control plots at most depths pre-treatment, became significantly more so post-treatment (Supporting Information Table S1). Drought plot Ψ_s did not recover following the wet periods of the 2007 and 2008 monsoons and spring 2008 (Fig. 2).

During both years, Ψ_{pd} and Ψ_{md} of both species declined during the spring/summer dry-down, reached minima in July and recovered during the monsoon season (Fig. 3). Comparisons on individual dates show that piñon Ψ_{pd} and Ψ_{md} were lower in the drought plot than the controls for the majority of 2008 (Fig. 3a,b). Juniper Ψ_{pd} and Ψ_{md} followed the same pattern, but were generally lower than piñon, and were more responsive to changes in Ψ_s than piñon (Figs 3 & 4).

We also observed, at the very end of the 2008 drought, piñon Ψ_{md} which on 2 d were less-negative than Ψ_{pd}. This occurred on all three plots, when Ψ_s was at the lowest values measured (Fig. 2) and E_s was also close to the minimum. The largest difference ($\Psi_{pd} - \Psi_{md} = \Delta\Psi$) was –0.73 MPa (Fig. 4 inset), and while the $\Delta\Psi$ standard error bars do not overlap with zero, that amount of a rise in Ψ_l during the day could still be within the measurement error. We discuss this pattern below.

Plant water use

Transpiration exhibited clear responses to the drought treatment. Drought plot piñon E_s was lower than either of the control plots' E_s, relative to pretreatment differences (Supporting Information Table S1 and Fig. 5a,b). The largest differences between drought and control piñon E_s occurred during times of relatively high water availability (Fig. 5a–c), that is, the end of the 2007 monsoon, early spring 2008 and the 2008 monsoon. Notably, the drought plot piñon had near-zero E_s ($E_s < 0.3$ mol m^{-2} s^{-2}) from February 2008 until they died in August 2008 (7 months). In contrast, control piñon E_s declined to near-zero in mid-April 2008 and started to rebound in July 2008, at the very beginning of the monsoon season and almost a month before drought plot piñon died (for a total time at minimum E_s of two and a half months). Diurnal patterns of E_s reveal a similar pattern (Supporting Information Fig. S3a): drought plot piñon had a lower daily maximum E_s and longer period with relatively low E_s. Thus, both the seasonal and diurnal time periods of relatively low gas exchange were extended in experimentally droughted piñon compared with controls. Drought plot juniper E_s was also significantly lower than either of the control plots post-treatment, relative to pretreatment differences (Supporting Information Table S1 and Fig. 5d,e). Similar to piñon, significant differences between drought and control plot juniper E_s were common during the monsoon periods and the early spring of 2008 (April–June, Fig. 5c–e).

Model results

The model calibration succeeded in fitting measured Ψ_{pd} in piñon ($r^2 = 0.82$) and juniper ($r^2 = 0.97$; Supporting Information Fig. S2). The use of measured E_s to predict Ψ_{pd} naturally yielded an excellent inverse prediction of E_{pred} ($r^2 = 0.980$ in piñon, $r^2 = 0.998$ in juniper), providing confidence in the model prediction of E_{crit}. Neither species on either plot was predicted to reach hydraulic failure, that is, $E_s \geq E_{crit}$. However, piñon approached E_{crit} much more closely than juniper, particularly in the drought plot (Figs 6a & 7). The smallest safety margins were observed during the pre-monsoon drought of 2007, when plant water potentials were at the lowest observed values.

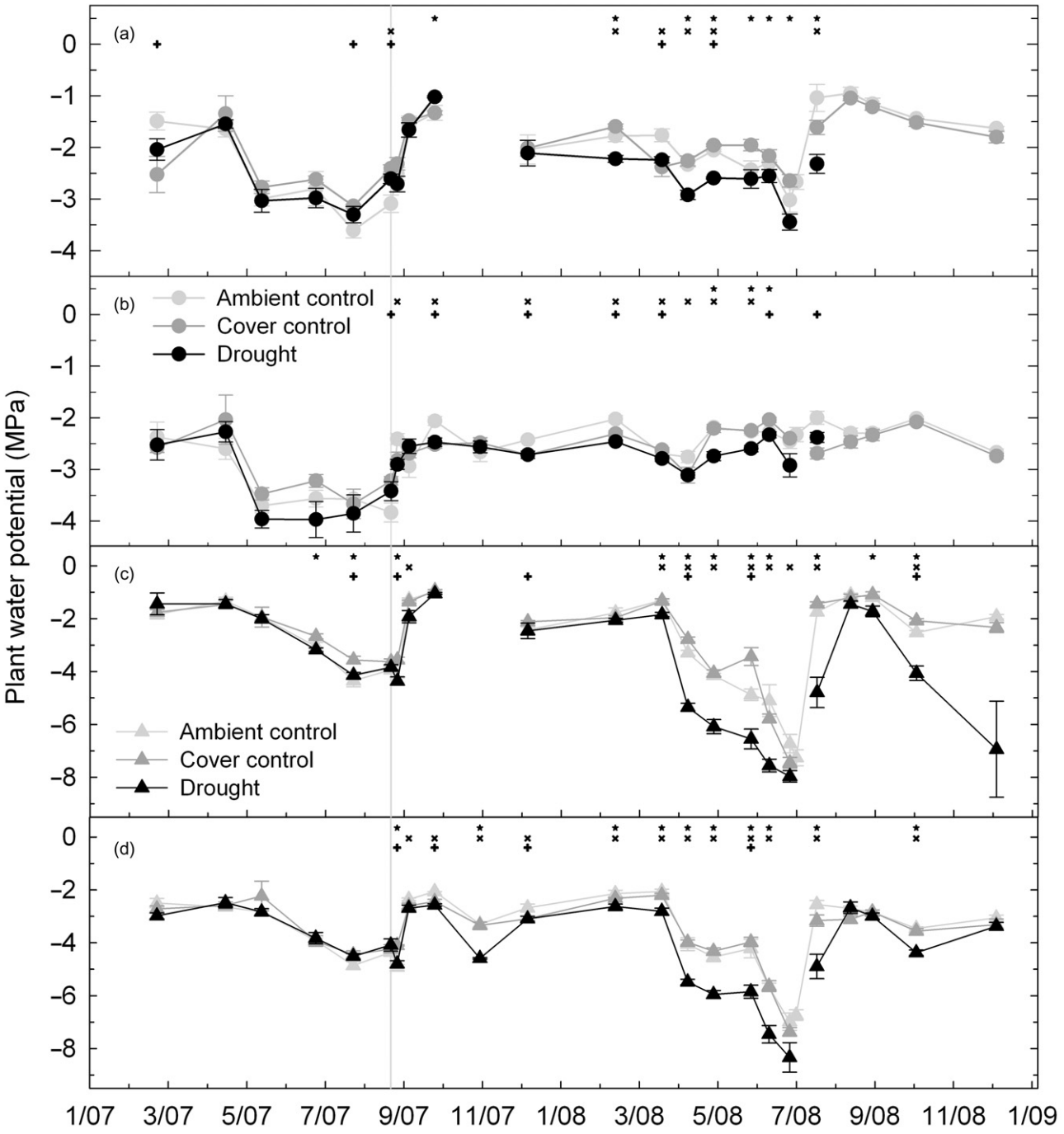

Figure 3. Plant water potentials: (a) piñon Ψ_{pd}, (b) piñon Ψ_{md}, (c) juniper Ψ_{pd} and (d) juniper Ψ_{md} for trees in the drought (black symbols), cover control (dark grey) and ambient control (light grey) treatments. Symbols are the means of five trees ± standard error for piñon (circles) and juniper (triangles). Differences between treatments significant at the $P = 0.05$ level are indicated for the comparisons between drought and cover control (★), drought and ambient control (×), and cover and ambient controls (+). Vertical lines indicate the initiation of treatments.

Modelled soil-to-canopy hydraulic conductance (K) was generally higher in piñon than juniper (Fig. 6b) within plot. Within species, K was markedly higher on the ambient plot than on the drought plot. Piñon on both plots experienced low K during the pre-monsoon period in 2007, prior to treatment installation. The monsoon coincided with infrastructure installation, and while K recovered in piñon on both plots, the increase was much greater in the ambient plot (Fig. 6b). The higher post-monsoon K in the ambient plot carried over to the following year, while K in the

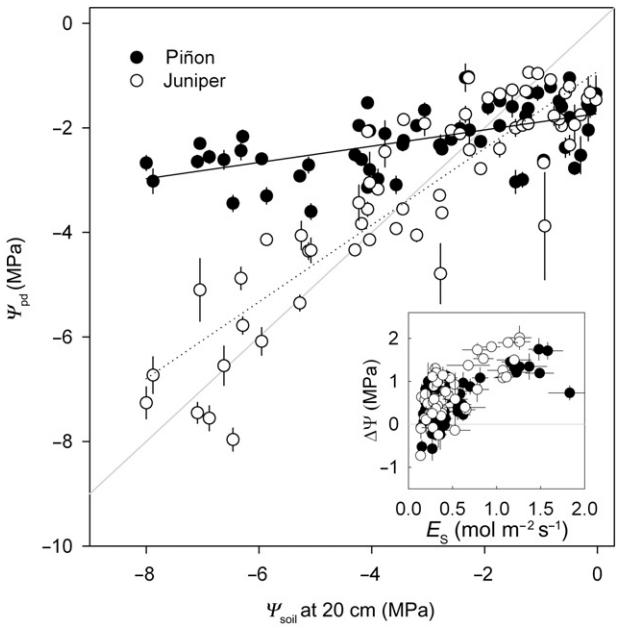

Figure 4. Ψ_{pd} response to Ψ_s (measured at 20 cm) for piñon (filled symbols, black line) and juniper (open symbols, dotted line). The 1:1 relationship is shown by the grey line. Inset shows $\Delta\Psi$ ($\Psi_{pd} - \Psi_{md}$) plotted against E_s with symbols as in the main figure. Error bars are standard error of the means. For piñon, $y = -1.73 + 0.156x$, $r^2 = 0.31$; for juniper, $y = -0.92 + 0.73x$, $r^2 = 0.78$.

drought plot stayed lower. Juniper did not exhibit a post-monsoon recovery of K in 2007 or 2008, and overall the treatment difference was less pronounced.

Despite the lack of outright hydraulic failure (Fig. 6a), piñon experienced a much greater loss of conductance during the study than juniper, and a treatment effect was seen in both species. Droughted piñon spent over 75% of the measurement days above 70% PLC, and 10% of days above 90% PLC (Fig. 8a). In contrast, the ambient piñon spent 60% of days below 40% PLC and less than 2% of days above 80% PLC, with an average of 43% PLC. Juniper exhibited much lower PLC than piñon, with no days over 50% PLC; PLC averaged 15% for ambient juniper and 38% for droughted juniper (Fig. 8b).

DISCUSSION

Piñon and juniper Ψ_l were consistent with isohydric and anisohydric stomatal regulation, respectively (Fig. 4), and the physiological responses of these species to ecosystem-scale manipulation of precipitation provided support for our hypotheses. Piñon mortality occurred after 11 months of drought treatment. During this time, soil water availability (Figs 2 & 3) and transpiration (Fig. 5) were substantially reduced. Consistent with our hypothesis, trees that died exhibited near-zero E_s for seven continuous months between treatment imposition and mortality, while piñon in other treatments, where no mortality occurred, exhibited similarly low E_s for c. 2 months (Fig. 5). The hydraulic model did not implicate hydraulic failure as the cause of mortality on the drought plot, but droughted piñon did experience greater loss of soil-canopy hydraulic conductance than ambient piñon and all juniper (Fig. 8). Despite its tight regulation of Ψ_l, piñon's modelled safety margin from E_{crit} was smaller than juniper's (Fig. 6a) within treatment.

Prolonged stomatal limitation of gas exchange and a more extensive loss of hydraulic conductance are both associated with mortality in this system, suggesting that both mechanisms interact to cause mortality (Sala, Piper & Hoch 2010; McDowell 2011). Droughted piñon exhibited chronically low soil-canopy hydraulic conductance relative to ambient trees, initially because of pretreatment differences in Ψ_l during the 2007 drought. Ironically, this pretreatment period was the closest the droughted trees came to hydraulic failure throughout the 2 years of measurement (Fig. 6a). The most critical effect of the rainout structures may have been to reduce the recovery response of the trees to the monsoon rains; low conductance in droughted piñon carried over into 2008. Over the period of measurement, droughted piñon spent more time with lower hydraulic conductance (Fig. 8), suggesting that hydraulic 'impairment' could have contributed to the observed mortality even if hydraulic failure did not occur outright. This hydraulic impairment is reflected in the amount of time spent at near-zero E_s (242 d for drought versus 46 d for cover control and 51 d for ambient control trees). This is a similar period of minimal gas exchange, and probable negative carbon balance, observed during piñon mortality in the same region in 2002–2003 (Breshears *et al*. 2009). Further, even before arriving at near-zero E_s, drought piñon experienced depressed E_s and likely lower storage of carbon relative to control plots (Fig. 5a, 9/07–10/07), meaning that drought piñon had lower carbon reserves going into a longer period of stomatal limitation. One likely connection between carbon limitation and hydraulic failure is the energetic demands of the processes required to re-establish hydraulic function (McDowell 2011), including, but not limited to, xylem refilling and production of new fine roots (Bucci *et al*. 2003; Gaul *et al*. 2008; Salleo *et al*. 2009; Zwieniecki & Holbrook 2009; Kitajima, Anderson & Allen 2010; Olesinski, Lavigne & Krasowski 2011). We speculate that any efforts by droughted piñon to recover hydraulic conductance would have resulted in an additional carbon cost at a time when K, E_s, and Ψ_l were all depressed relative to the controls.

Comparison of results to carbon starvation and hydraulic failure hypotheses

Inasmuch as E_s is a proxy for carbon gain, our results are consistent with drought constraining piñon carbon balance in a way that predisposed those trees to successful colonization by bark beetles (Martinez-Vilalta, Pinol & Beven 2002; McDowell *et al*. 2008; Breshears *et al*. 2009). Piñon has been shown to experience zero net assimilation at water potentials of –2.3 MPa or lower (Lajtha & Barnes 1991). In our experiment, in the 347 d between treatment imposition

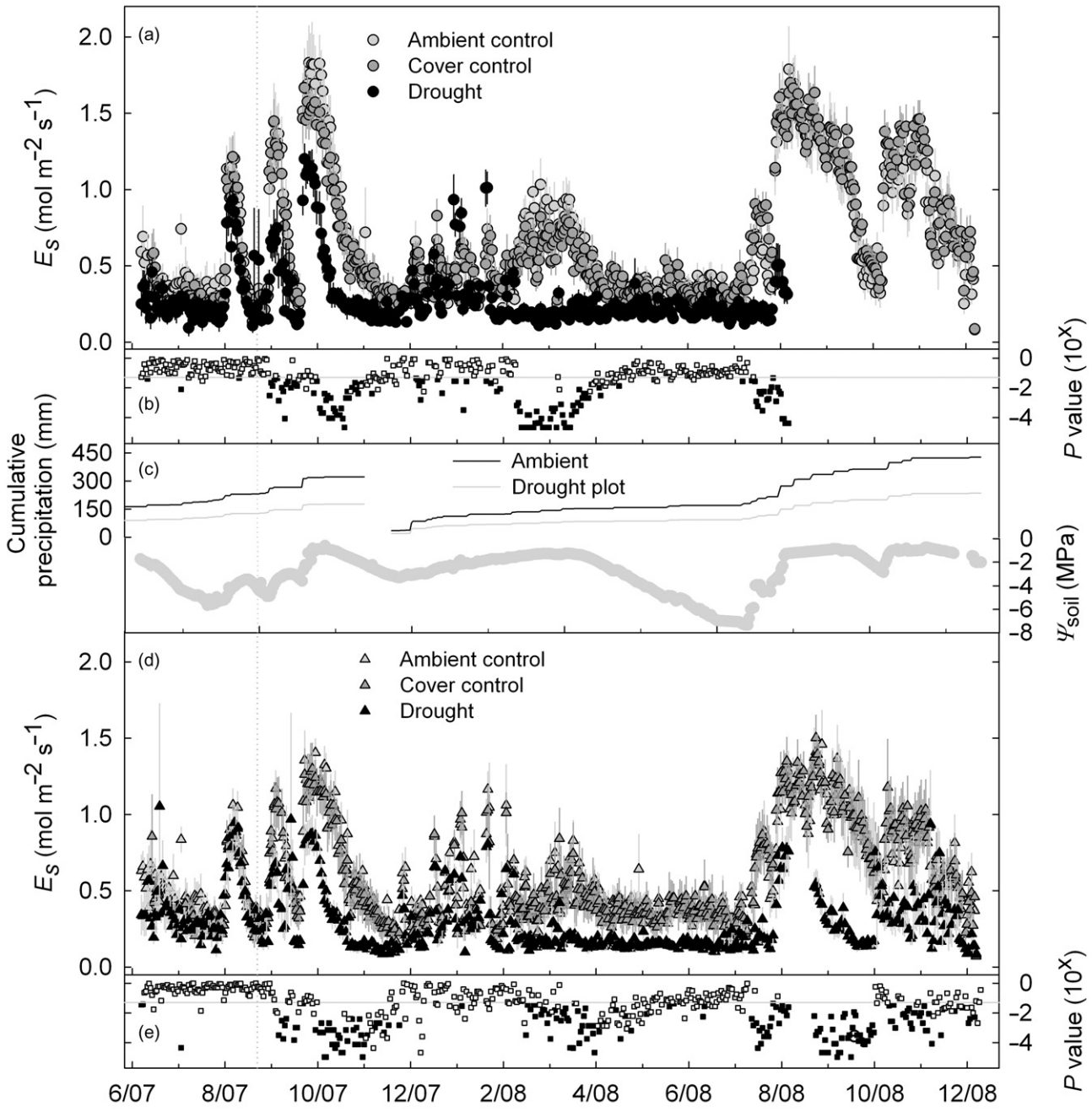

Figure 5. Time series of treatment effect on plant transpiration (E_s) in (a) piñon pine and (d) juniper. Symbols are the means of five trees ± standard error of the mean for drought (black), cover control (dark grey) and ambient control (light grey) treatments. *t*-Test results for comparisons of daily maximum E_s are shown in (b) and (e), where drought plot is significantly different from ambient control (below horizontal line, which represents $P = 0.05$), ambient and cover controls (filled symbols) or neither of the controls (opens symbols above horizontal line). Panel (c) shows cumulative precipitation at the micrometeorological station (black line) and as calculated in the drought plot (grey line), and ambient control plot Ψ_s at 40–100 cm depth. Dotted vertical line indicates initiation of treatments.

and the onset of piñon mortality, drought plot piñon experienced 250 d (or 72%) when none of the measured soil layers were above –2.3 MPa. Cover control piñon experienced 95 d (27%) and ambient control piñon experienced 130 d (37%) during the same interval. Thus, while piñon under ambient field conditions experience a certain number of days each year when carbon assimilation is likely impossible, our drought treatment significantly extended that period of time with consequences for tree survival. Concurrent direct measurements of native xylem embolism with plant carbon balance, including phloem transport, are required to directly address hydraulic failure and carbon starvation hypotheses (Sala *et al*. 2010; McDowell 2011; Ryan 2011; Hudson *et al*., unpublished manuscript).

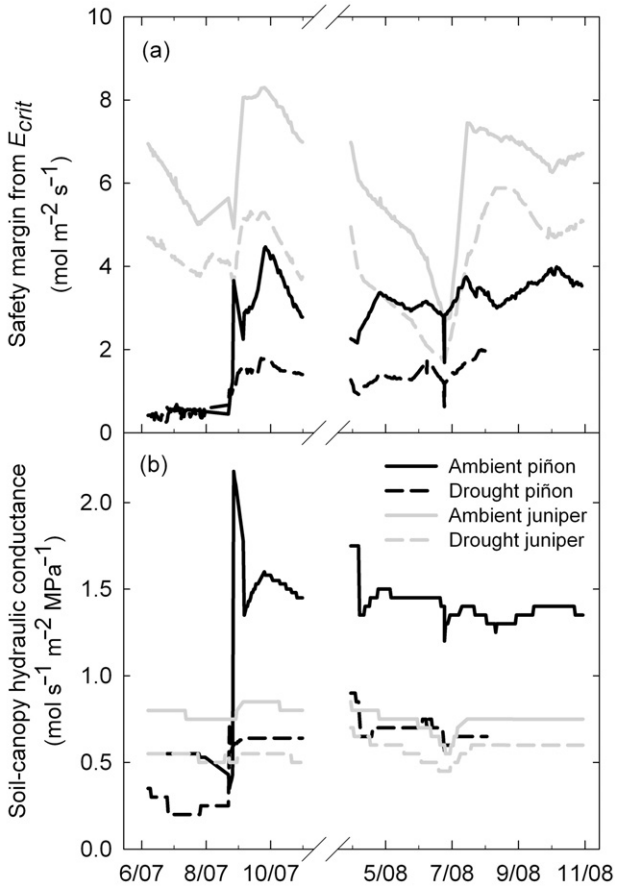

Figure 6. Time series of soil-canopy hydraulic conductance (a) and the safety margin between E_s and E_{crit} (b) for piñon (black lines) and juniper (grey lines) on the ambient (solid) and drought (dashed) plots.

While prolonged periods of near-zero E_s are consistent with unfavourable carbon balance contributing to mortality, an alternate hypothesis is that the defence response against bark beetles was limited by low cellular water potentials in trees that died (Fig. 3). The low tissue water potentials observed in the drought piñon could constrain the autonecrotic responses that exclude beetles from successful entry (Kolb *et al*. 2007; McDowell *et al*. 2011). While it seems clear that carbon and hydraulic constraints to survival were both involved in piñon mortality, further research is required to test how these factors influence the defensive response during severe drought (Gaylord *et al*., unpublished data).

The added severity of the experimental drought treatment was physiologically significant for juniper because, unlike piñon, it was not already maximally stressed under ambient seasonal drought. The close association between measured Ψ_s and juniper Ψ_{pd} (Fig. 4) indicates that juniper is hydraulically connected to the soil layers we measured. While juniper's greater cavitation resistance may prevent it from completely losing hydraulic conductance under even extreme experimental drought conditions, the temporal and magnitude differences between drought and control treatment E_s on seasonal (Fig. 5) and diurnal (Supporting Information Fig. S3b) timescales suggest that experimentally droughted juniper may also be experiencing depressed carbon uptake. Leaf-level measurements confirm this prediction of lower net photosynthesis in both species under drought treatments (Limousin *et al*., unpublished data). Over extended periods, limits to carbon availability can lead to susceptibility to biotic attack by insects, fungi or bacteria as a proximal mechanism of mortality (Guarin & Taylor 2005; Millar, Westfall & Delany 2007; Greenwood & Weisberg 2008). As juniper lacks an insect pathogen with an effect equivalent to that of *I. confusus* in piñon, juniper mortality may only occur when hydraulic failure and/or carbon limitation progress to metabolic dysfunction.

Our results are counter to the prediction that anisohydric species like juniper would be at greater risk of hydraulic failure than isohydric species (McDowell *et al*. 2008). The safety margin between modelled E_{crit} and measured E_s was consistently positive for juniper (Fig. 6a) and, within plot, greater than piñon's safety margin. However, despite its cavitation resistance (e.g. Pockman & Sperry 2000; West *et al*. 2007b; McDowell *et al*. 2008; Willson *et al*. 2008) and deep rooting (Foxx & Tierney 1987; West *et al*. 2007a), juniper appears unable to recover hydraulic conductance following drought (Fig. 6b). This result is consistent with the literature for *Juniperus osteosperma* (West *et al*. 2007b). Soil drought sufficient for juniper to experience hydraulic failure may require multiple years of treatment to develop.

Anomalous plant water potential measurements

Pre-dawn plant water potentials more negative than midday water potentials ($\Psi_{pd} < \Psi_{md}$) are not commonly

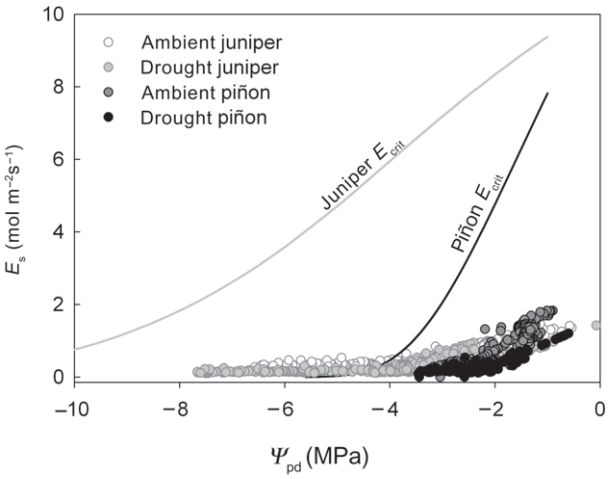

Figure 7. Maximum 'envelopes' for steady-state sap flow per sapwood area (E_{crit}) as a function of pre-dawn water potential. Curves indicate maximum values based on the maximum K_{sat} required for model calibration across years and treatments for each species (juniper, grey; piñon, black). Data points represent individual measurement days during the 2 years of monitoring for both ambient and droughted plots (juniper: open symbols, ambient control; light grey, drought; piñon: dark grey, ambient control; black, drought).

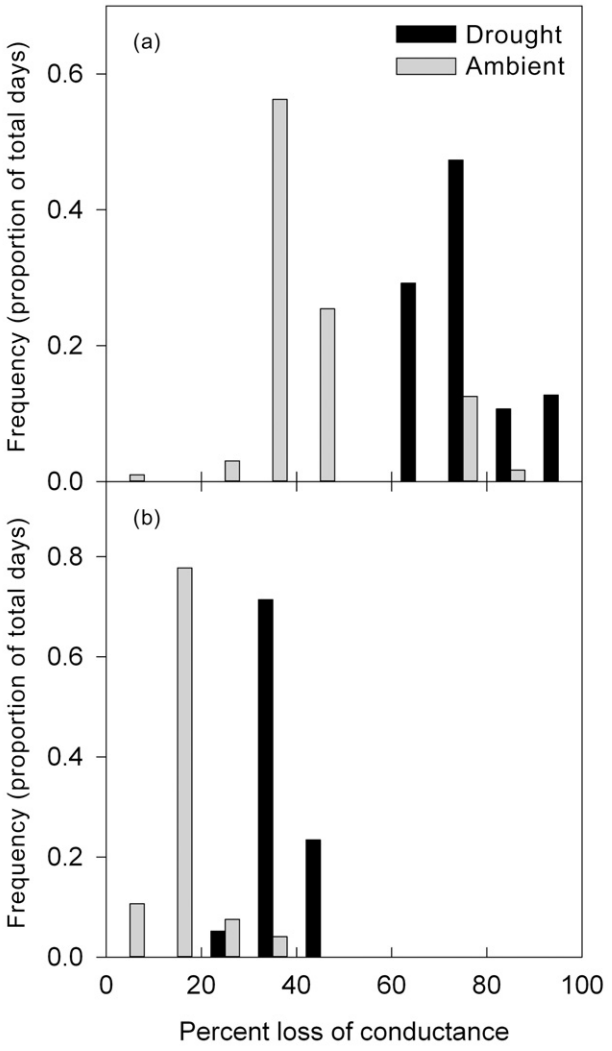

Figure 8. Frequency of measurement days spent at 10% classes of percent loss of conductance (PLC) for (a) piñon and (b) juniper in the ambient (grey) and drought (black) plots. Bars are paired within each 10% PLC class from 0 to 100%. The PLC for each species was calculated relative to the single maximum K_{sat} required for model calibration over both treatments and years.

presented, though this pattern has been reported in the literature (e.g. Syvertsen, Cunningham & Feather 1975; Radosevich & Conard 1980; Baker, Rundel & Parsons 1982; BassiriRad *et al*. 1999). We observed this pattern during the driest periods of measurement, consistent with the observations of Radosevich & Conard (1980), when plant water potentials were very low and E_s was near zero (Fig. 4 inset). One explanation is the daytime condensation of water vapour in the rhizosphere driven by diurnal thermal gradients in the soil (Syvertsen *et al*. 1975). It is also possible that roots refill at night and re-establish contact with dry soils, then cavitate during the day (resulting in hydraulic isolation) and therefore do not reflect the water potential of the soils to which they were previously connected (Sperry & Hacke 2002). Night-time transpiration is another explanation, but one that we can exclude based on subsequent porometer measurements (data not shown). Finally, it is possible that hydraulic redistribution is occurring at night, and that the Ψ of the canopy (represented by Ψ_{pd}) is equilibrated with the root crown Ψ, which is somewhere along the flow path between the very dry surface soils and wetter deep soils. This phenomenon warrants further investigation, but unfortunately during the acquisition of this dataset we did not have appropriate instrumentation in place (i.e. bidirectional sap flow sensors, sap flow sensors in roots or stem psychrometers on roots). The hydraulic model we employed is not parameterized to predict this phenomenon over the time scale of interest (i.e. a single day).

Model performance

Performance of the hydraulic model was limited by three main factors: first, we did not have information about the cavitation vulnerability of leaf and fine root xylem, which has been shown to be more limiting than branch and coarse root xylem in many conifer species (Hacke *et al*. 2000; Brodribb & Cochard 2009). The inclusion of more-vulnerable xylem components in the model would narrow the safety margins for each species.

Second, the relationship between target tree rooting patterns and the location/depth of the soil psychrometers was unknown. Juniper appeared better coupled to the soil we measured with psychrometers than piñon (Fig. 4), but preliminary efforts to parameterize the model with measured Ψ_s still failed when Ψ_{md} was less negative than Ψ_s. Observations of $\Psi_{md} > \Psi_s$ may be evidence of hydraulic isolation, which might occur if fine roots in contact with very dry soil die or cavitate. During this period, the oxygen isotope ratio of xylem sap was substantially enriched relative to any source water, further supporting the plausibility of hydraulic isolation (Yepez *et al*., unpublished manuscript). Theoretically, the isohydric strategy combined with hydraulic isolation can result in plant water potentials which are less negative than Ψ_s. If stomata close to prevent hydraulic failure, and fine root death/cavitation results in hydraulic isolation, then the plant is essentially a closed container, evaporating through its cuticle but otherwise conserving its water potential independent of the soil (Breshears *et al*. 2009; Sevanto *et al*., unpublished data). Positive sap flow measurements during this time contradict complete hydraulic isolation, however, and deep roots have been shown to be an important source of water in a variety of environments (e.g. Markewitz *et al*. 2010). Ultimately, the preponderance of evidence suggested that trees at this site had access to soil compartments deeper and wetter than those measured directly, so Ψ_{pd} was used as an integrated measure of the soils to which the trees were hydraulically connected.

Finally, there is a degree of uncertainty regarding measurements made with thermal dissipation probes which would confound efforts to fit modelled E_{pred} to measured E_s. Most relevant to our conclusions, the probes may overestimate low sap flow (Burgess, Adams & Bleby 2000; Burgess *et al*. 2001; Pangle, unpublished data), and

it is also possible that the minimum measured E_s may be a function of phloem-driven circulation rather than transpiration-driven water loss (Hölttä *et al*. 2006; McDowell & Sevanto 2010). We also did not measure radial variation in sap flux density, but we are not scaling to whole tree or stand water use, and sap flux density tends to be greater closer to the cambium (Cohen *et al*. 2008). Accounting for the lower sap flux density, either because of radial variation or poor sensitivity at low flows, would lower the average E_s; fitting E_{pred} to lower E_s would likely lower E_{crit} as well. It is difficult to tell whether this would result in predicted hydraulic failure because both parameters would shift in the same direction.

Ecosystem manipulation performance

The drought manipulation study described here was particularly effective for some aspects of the study of mortality mechanisms. Perhaps the most critical value of this study is that most of the piñon trees in the drought treatment died; very few studies of drought effects arrive at that endpoint, which greatly limits our ability to infer mortality mechanisms (McDowell & Sevanto 2010). An additional value of the study is that our drought treatment accurately imitated the impact on piñon Ψ_{pd} of the 2000–2003 regional drought in southwestern United States that resulted in widespread piñon mortality. The 2002 piñon mortality event followed 10 months with Ψ_{pd} below –2 MPa and an associated negative carbon balance (Breshears *et al*. 2005, 2009). Our experimental drought produced Ψ_{pd} at or below the threshold for zero carbon gain for a total of 8 months, in comparison with only 6 months for the control plots (Fig. 3).

The manipulation described here also has limitations for the study of mortality mechanisms. Though we effectively manipulated soil water during drought, we did not intentionally or systematically manipulate temperature (Pangle *et al*., 2012). Drought typically results in both reduced precipitation and elevated temperatures (Breshears *et al*. 2005), and the latter may be a critical driver of mortality through its impacts on respiration and VPD (McDowell *et al*. 2008; Adams *et al*. 2009). To truly discriminate between mortality mechanisms, one must understand not only hydraulic limits, but also the carbon balance of trees including non-structural carbohydrates, phloem transport and defence compounds (Hölttä *et al*. 2009; McDowell & Sevanto 2010; Sala *et al*. 2010). Studies to address all of these aspects are ongoing and will provide valuable insight into mortality mechanisms.

ACKNOWLEDGMENTS

We gratefully acknowledge the efforts of Jim Elliot, Monica Gaylord, Julie Glaser, Jennifer Johnson, Sam Markwell, Clif Meyer, Matt Spinelli and numerous undergraduate assistants in the implementation of this experiment and collection of much of the data. Rosie Fisher, Sanna Sevanto, Jean-Marc Limousin and two anonymous reviewers provided valuable input. This project was supported by an award to N.G.M. and W.T.P. from the Department of Energy's Office of Science (BER) and to J.A.P. by the National Science Foundation's Graduate Research Fellowship Program. The project was also supported by the resources and staff of the Sevilleta LTER (funded by NSF DEB 0620482) and Sevilleta Field Station at the University of New Mexico.

REFERENCES

Adams H.D., Guardiola-Claramonte M., Barron-Gafford G.A., Villegas J.C., Breshears D.D., Zou C.B., Troch P.A. & Huxman T.E. (2009) Temperature sensitivity of drought-induced tree mortality portends increased regional die-off under global-change-type drought. *Proceedings of the National Academy of Sciences of the United States of America* **106,** 7063–7066.

Allen C.D., Macalady A.K., Chenchouni H., *et al*. (2010) A global overview of drought and heat-induced tree mortality reveals emerging climate change risks for forests. *Forest Ecology and Management* **259,** 660–684.

Baker G.A., Rundel P.W. & Parsons D.J. (1982) Comparative phenology and growth in three chaparral shrubs. *Botanical Gazette* **143,** 94–100.

BassiriRad H., Tremmel D.C., Virginia R.A., Reynolds J.F., de Soyza A.G. & Brunell M.H. (1999) Short-term patterns in water- and nitrogen acquisition by two desert shrubs following a simulated summer rain. *Plant Ecology* **145,** 27–36.

Bigler C., Gavin D.G., Gunning C. & Veblen T.T. (2007) Drought induces lagged tree mortality in a subalpine forest in the Rocky Mountains. *Oikos* **116,** 1983–1994.

Bonal D., Bosc A., Ponton S., *et al*. (2008) Impact of severe dry season on net ecosystem exchange in the Neotropical rainforest of French Guiana. *Global Change Biology* **14,** 1917–1933.

Breshears D.D., Cobb N.S., Rich P.M., *et al*. (2005) Regional vegetation die-off in response to global-change-type drought. *Proceedings of the National Academy of Sciences of the United States of America* **102,** 15144–15148.

Breshears D.D., Myers O.B., Meyer C.W., Barnes F.J., Zou C.B., Allen C.D., Mcdowell N.G. & Pockman W.T. (2009) Tree die-off in response to global change-type drought: mortality insights from a decade of plant water potential measurements. *Frontiers in Ecology and the Environment* **7,** 185–189.

Brodribb T.J. & Cochard H. (2009) Hydraulic failure defines the recovery and point of death in water-stressed conifers. *Plant Physiology* **149,** 575–584.

Brodribb T.J. & Holbrook N.M. (2003) Changes in leaf hydraulic conductance during leaf shedding in seasonally dry tropical forest. *New Phytologist* **158,** 295–303.

Bucci S.J., Scholz F.G., Goldstein G., Meinzer F.C. & Sternberg L. da S.L. (2003) Dynamic changes in hydraulic conductivity in petioles of two savanna tree species: factors and mechanisms contributing to the refilling of embolized vessels. *Plant, Cell & Environment* **26,** 1633–1645.

Burgess S.S.O., Adams M.A. & Bleby T.M. (2000) Measurement of sap flow in roots of woody plants: a commentary. *Tree Physiology* **20,** 909–913.

Burgess S.S.O., Adams M.A., Turner N.C., Beverly C.R., Ong C.K., Khan A.A.H. & Bleby T.M. (2001) An improved heat pulse method to measure low and reverse rates of sap flow in woody plants. *Tree Physiology* **21,** 589–598.

Bush S.E., Hultine K.R., Sperry J.S. & Ehleringer J.R. (2010) Calibration of thermal dissipation sap flow probes for ring- and diffuse-porous trees. *Tree Physiology* **30,** 1545–1554.

Campbell G.S. (1985) *Soil Physics with Basic; Transport Models for Soil-Plant Systems*. Elsevier Science Publishers, Amsterdam.

Chansler J.F. (1964) *Overwintering Habits of Ips Lecontei Sw. and Ips Confusus (Lec.) in Arizona and New Mexico*. U.S. Department of Agriculture Forest Service, Rocky Mountain Forest and Range Experiment Station, Fort Collins, CO.

Clearwater M.J., Meinzer F.C., Andrade J.L., Goldstein G. & Holbrook N.M. (1999) Potential errors in measurement of nonuniform sap flow using heat dissipation probes. *Tree Physiology* **19,** 681–687.

Cochard H. (2002) A technique for measuring xylem hydraulic conductance under high negative pressures. *Plant, Cell & Environment* **25,** 815–819.

Cochard H., Coll L., Le Roux X. & Ameglio T. (2002) Unraveling the effects of plant hydraulics on stomatal closure during water stress in walnut. *Plant Physiology* **128,** 282–290.

Cochard H., Damour G., Bodet C., Tharwat I., Poirier M. & Ameglio T. (2005) Evaluation of a new centrifuge technique for rapid generation of xylem vulnerability curves. *Physiologia Plantarum* **124,** 410–418.

Cohen Y., Cohen S., Cantuarias-Aviles T. & Schiller G. (2008) Variations in the radial gradient of sap velocity in trunks of forest and fruit trees. *Plant and Soil* **305,** 49–59.

Domec J.-C., King J.S., Noormets A., Treasure E., Gavazzi M.J., Sun G. & McNulty S.G. (2010) Hydraulic redistribution of soil water by roots affects whole-stand evapotranspiration and net ecosystem carbon exchange. *New Phytologist* **187,** 171–183.

Ewers B.E., Oren R. & Sperry J.S. (2000) Influence of nutrient versus water supply on hydraulic architecture and water balance in *Pinus taeda*. *Plant, Cell & Environment* **23,** 1055–1066.

Fensham R.J., Fairfax R.J. & Ward D.P. (2009) Drought-induced tree death in savanna. *Global Change Biology* **15,** 380–387.

Floyd M.L., Clifford M., Cobb N.S., Hanna D., Delph R., Ford P. & Turner D. (2009) Relationship of stand characteristics to drought-induced mortality in three Southwestern piñon-juniper woodlands. *Ecological Applications* **19,** 1223–1230.

Foxx T.S. & Tierney G.D. (1987) Rooting patterns in the pinyon-juniper woodland. Proceedings: pinyon–juniper conference, pp. 69–79. U.S. Department of Agriculture, Forest Service, Intermountain Research Station, Reno, NV, USA.

Friedlingstein P., Cox P., Betts R., *et al*. (2006) Climate-carbon cycle feedback analysis: results from the (CMIP)-M-4 model intercomparison. *Journal of Climate* **19,** 3337–3353.

Galvez D.A. & Tyree M.T. (2009) Impact of simulated herbivory on water relations of aspen (*Populus tremuloides*) seedlings: the role of new tissue in the hydraulic conductivity recovery cycle. *Oecologia* **161,** 665–671.

Gaul D., Hertel D., Borken W., Matzner E. & Leuschner C. (2008) Effects of experimental drought on the fine root system of mature Norway spruce. *Forest Ecology and Management* **256,** 1151–1159.

van Genuchten M.T. (1980) A closed-form equation for predicting the hydraulic conductivity of unsaturated soils. *Soil Science Society of America Journal* **44,** 892–898.

Goulden M.L. & Field C.B. (1994) Three methods for monitoring the gas exchange of individual tree canopies – ventilated-chamber, sap-flow and Penman-Monteith measurements on evergreen oaks. *Functional Ecology* **8,** 125–135.

Granier A. (1987) Evaluation of transpiration in a Douglas-fir stand by means of sap flow measurements. *Tree Physiology* **3,** 309–319.

Greenwood D.L. & Weisberg P.J. (2008) Density-dependent tree mortality in pinyon-juniper woodlands. *Forest Ecology and Management* **255,** 2129–2137.

Guarin A. & Taylor A.H. (2005) Drought triggered tree mortality in mixed conifer forests in Yosemite National Park, California, USA. *Forest Ecology and Management* **218,** 229–244.

Hacke U.G., Sperry J.S., Ewers B.E., Ellsworth D.S., Schafer K.V.R. & Oren R. (2000) Influence of soil porosity on water use in *Pinus taeda*. *Oecologia* **124,** 495–505.

Hölttä T., Vesala T., Sevanto S., Perämäki M. & Nikenmaa E. (2006) Modeling xylem and phloem water flows in trees according to cohesion theory and Münch hypothesis. *Trees* **20,** 67–78.

Hölttä T., Cochard H., Nikinmaa E. & Mencuccini M. (2009) Capacitive effect of cavitation in xylem conduits: results from a dynamic model. *Plant, Cell & Environment* **32,** 10–21.

Horner G.J., Baker P.J., Mac Nally R., Cunningham S.C., Thomson J.R. & Hamilton F. (2009) Mortality of developing floodplain forests subjected to a drying climate and water extraction. *Global Change Biology* **15,** 2176–2186.

Iovi K., Kolovou C. & Kyparissis A. (2009) An ecophysiological approach of hydraulic performance for nine Mediterranean species. *Tree Physiology* **29,** 889–900.

IPCC (2007) Climate Change 2007: The physical science basis. Contribution of Working Group I to the Fourth Assessment Report of the Intergovernmental Panel on Climate Change. pp. 1009. Cambridge University Press, Cambridge.

Kaufmann M.R. & Thor G.L. (1982) Measurement of water stress in subalpine trees: effects of temporary tissue storage methods and needle age. *Canadian Journal of Forest Research-Revue Canadienne De Recherche Forestiere* **12,** 969–972.

Kitajima K., Anderson K.E. & Allen M.F. (2010) Effect of soil temperature and soil water content on fine root turnover rate in a California mixed conifer ecosystem. *Journal of Geophysical Research* **115,** G04032.

Kolb T.E., Holmberg K.M., Wagner M.R. & Stone J.E. (1998) Regulation of ponderosa pine foliar physiology and insect resistance mechanisms by basal area treatments. *Tree Physiology* **18,** 375–381.

Kolb T.E., Agee J.K., Fulé P.Z., McDowell N.G., Pearson K., Sala A. & Waring R.H. (2007) Perpetuating old ponderosa pine. *Forest Ecology and Management* **249,** 141–157.

Lajtha K. & Barnes F.J. (1991) Carbon gain and water-use in pinyon pine-juniper woodlans of northern New Mexico – field versus phytotron chamber measurements. *Tree Physiology* **9,** 59–67.

Li Y.Y., Sperry J.S., Taneda H., Bush S.E. & Hacke U.G. (2008) Evaluation of centrifugal methods for measuring xylem cavitation in conifers, diffuse- and ring-porous angiosperms. *New Phytologist* **177,** 558–568.

Linton M.J., Sperry J.S. & Williams D.G. (1998) Limits to water transport in *Juniperus osteosperma* and *Pinus edulis*: implications for drought tolerance and regulation of transpiration. *Functional Ecology* **12,** 906–911.

Markewitz D., Devine S., Davidson E.A., Brando P. & Nepstad D.C. (2010) Soil moisture depletion under simulated drought in the Amazon: impacts on deeproot uptake. *New Phytologist* **187,** 592–607.

Martinez-Vilalta J., Pinol J. & Beven K. (2002) A hydraulic model to predict drought-induced mortality in woody plants: an application to climate change in the Mediterranean. *Ecological Modeling* **155,** 127–147.

McDowell N., Pockman W.T., Allen C.D., *et al*. (2008) Mechanisms of plant survival and mortality during drought: why do some plants survive while others succumb to drought? *New Phytologist* **178,** 719–739.

McDowell N.G. (2011) Mechanisms linking drought, hydraulics, carbon metabolism, and vegetation mortality. *Plant Physiology* **155,** 1051–1059.

McDowell N.G. & Sevanto S. (2010) The mechanisms of carbon starvation: how, when, or does it even occur at all? *New Phytologist* **186,** 264–266.

McDowell N.G., Beerling D.J., Breshears D.D., Fisher R.A., Raffa K.F. & Stitt M. (2011) The interdependence of mechanisms underlying climate-driven vegetation mortality. *Trends in Ecology and Evolution* **26,** 523–532.

Millar C.I., Westfall R.D. & Delany D.L. (2007) Response of high-elevation limber pine (*Pinus flexilis*) to multiyear droughts and 20th-century warming, Sierra Nevada, California, USA. *Canadian Journal of Forest Research-Revue Canadienne De Recherche Forestiere* **37,** 2508–2520.

Neufeld H.S., Grantz D.A., Meinzer F.C., Goldstein G., Crisosto G.M. & Crisosto C. (1992) Genotypic variability in vulnerability of leaf xylem to cavitation in water-stressed and well-irrigated sugarcane. *Plant Physiology* **100,** 1020–1028.

Olesinski J., Lavigne M.B. & Krasowski M.J. (2011) Effects of soil moisture manipulations on fine root dynamics in a mature balsam fir (*Abies balsamea* L. Mill.) forest. *Tree Physiology* **31,** 339–348.

Pangle R.E., Hill J.P., Plaut J.A., Yepez E.A., Elliot J.R., Gehres N., McDowell N.G. & Pockman W.T. (2012) Methodology and performance of a rainfall manipulation experiment in a piñon-juniper woodland. *Ecosphere* **3,** 28. URL http://dx.doi.org/10.1890/ES11-00369.1.

Phillips N. & Oren R. (2001) Intra- and inter-annual variation in transpiration of a pine forest. *Ecological Applications* **11,** 385–396.

Pockman W.T. & Sperry J.S. (2000) Vulnerability to xylem cavitation and the distribution of Sonoran desert vegetation. *American Journal of Botany* **87,** 1287–1299.

R Development Core Team (2008) *R: A Language and Environment for Statistical Computing*. R Foundation for Statistical Computing, Vienna, Austria.

Radosevich S.R. & Conard S.G. (1980) Physiological control of chamise shoot growth after fire. *American Journal of Botany* **67,** 1442–1447.

Resco V., Ewers B.E., Sun W., Huxman T.E., Weltzin J.F. & Williams D.G. (2009) Drought-induced hydraulic limitations constrain leaf gas exchange recovery after precipitation pulses in the C-3 woody legume, *Prosopis velutina*. *New Phytologist* **181,** 672–682.

Ryan M.G. (2011) Tree responses to drought. *Tree Physiology* **31,** 237–239.

Sala A., Piper F. & Hoch G. (2010) Physiological mechanisms of drought-induced tree mortality are far from being resolved. *New Phytologist* **186,** 274–281.

Salleo S., Trifilò P., Esposita S., Nardini A. & Lo Gullo M.A. (2009) Starch-to-sugar conversion in wood parenchyma of field-growing *Laurus nobilis* plants: a component of the signal pathway for embolism repair? *Functional Plant Biology* **36,** 815–825.

Sitch S., Huntingford C., Gedney N., *et al*. (2008) Evaluation of the terrestrial carbon cycle, future plant geography and climate-carbon cycle feedbacks using five Dynamic Global Vegetation Models (DGVMs). *Global Change Biology* **14,** 2015–2039.

Snyder K.A., Richards J.H. & Donovan L.A. (2003) Night-time conductance in C-3 and C-4 species: do plants lose water at night? *Journal of Experimental Botany* **54,** 861–865.

Sparks J.P. & Black R.A. (1999) Regulation of water loss in populations of *Populus trichocarpa*: the role of stomatal control in preventing xylem cavitation. *Tree Physiology* **19,** 453–459.

Sperry J.S. & Hacke U.G. (2002) Desert shrub water relations with respect to soil characteristics and plant function type. *Functional Ecology* **16,** 367–378.

Sperry J.S., Donnelly J.R. & Tyree M.T. (1988) A method for measuring hydraulic conductivity and embolism in xylem. *Plant, Cell & Environment* **11,** 35–40.

Sperry J.S., Adler F.R., Campbell G.S. & Comstock J.P. (1998) Limitation of plant water use by rhizosphere and xylem conductance: results from a model. *Plant, Cell & Environment* **21,** 347–359.

Sperry J.S., Hacke U.G., Oren R. & Comstock J.P. (2002) Water deficits and hydraulic limits to leaf water supply. *Plant, Cell & Environment* **25,** 251–263.

Stone J.E., Kolb T.E. & Covington W.W. (1999) Effects of restoration thinning on presettlement *Pinus ponderosa* in northern Arizona. *Restoration Ecology* **7,** 172–182.

Suarez M.L., Ghermandi L. & Kitzberger T. (2004) Factors predisposing episodic drought-induced tree mortality in *Nothofagus* – site, climatic sensitivity and growth trends. *Journal of Ecology* **92,** 954–966.

Syvertsen J.P., Cunningham G.L. & Feather T.V. (1975) Anomalous diurnal patterns of stem xylem water potentials in *Larrea tridentata*. *Ecology* **56,** 1423–1428.

Tardieu F. & Simonneau T. (1998) Variability among species of stomatal control under fluctuating soil water status and evaporative demand: modelling isohydric and anisohydric behaviours. *Journal of Experimental Botany* **49,** 419–432.

Tyree M.T. & Sperry J.S. (1988) Do woody plants operate near the point of catastrophic xylem dysfunction caused by dynamic water stress – answers from a model. *Plant Physiology* **88,** 574–580.

West A.G., Hultine K.R., Burtch K.G. & Ehleringer J.R. (2007a) Seasonal variations in moisture use in a pinon-juniper woodland. *Oecologia* **153,** 787–798.

West A.G., Hultine K.R., Jackson T.L. & Ehleringer J.R. (2007b) Differential summer water use by *Pinus edulis* and *Juniperus osteosperma* reflects contrasting hydraulic characteristics. *Tree Physiology* **27,** 1711–1720.

West A.G., Hultine K.R., Sperry J.S., Bush S.E. & Ehleringer J.R. (2008) Transpiration and hydraulic strategies in a pinon-juniper woodland. *Ecological Applications* **18,** 911–927.

Willson C.J., Manos P.S. & Jackson R.B. (2008) Hydraulic traits are influenced by phylogenetic history in the drought-resistant, invasive genus *Juniperus* (Cupressaceae). *American Journal of Botany* **95,** 299–314.

Wood S.L. (1982) *The Bark and Ambrosia Beetles of North and Central America (Coleoptera: Scolytidae), A Taxonomic Monograph*. Brigham Young University, Provo, UT.

Worrall J.J., Egeland L., Eager T., Mask R.A., Johnson E.W., Kemp P.A. & Shepperd W.D. (2008) Rapid mortality of *Populus tremuloides* in southwestern Colorado, USA. *Forest Ecology and Management* **255,** 686–696.

Zwieniecki M.A. & Holbrook N.M. (2009) Confronting Maxwell's demon: biophysics of xylem embolism repair. *Trends in Plant Science* **14,** 530–534.

Received 13 March 2011; received in revised form 27 February 2012; accepted for publication 20 March 2012

SUPPORTING INFORMATION

Additional Supporting Information may be found in the online version of this article:

Figure S1. Photos depicting (a) drought plot on 8/21/2008 showing troughs draining to gutter, (b) cover control plot on 7/28/2007 and (c) piñon mortality in the drought plot on 10/22/2008. Photo credit: J. Hill (a,b) and J. Plaut (c).

Figure S2. Modelled versus measured pre-dawn water potential compared across both plots and years (2007–2008)

for piñon (solid symbols, black line) and juniper (open symbols, grey line). The 1:1 line (dotted) is shown for comparison. Data points represent plot means. Piñon $r^2 = 0.82$; juniper $r^2 = 0.97$.

Figure S3. Piñon (a) and juniper (b) diurnal E_s averaged over the 10 d period June 21–June 30, 2008 for drought (filled symbols) and ambient control (open symbols) treatments. Grey line indicates photosynthetically active radiation (PAR); black line indicates vapour pressure deficit (VPD). Data points represent plot means and all error bars represent the standard error of the mean.

Table S1. Comparisons of pretreatment and post-treatment differences between plot means for soil water potentials (Ψ_s, MPa), plant water potentials (Ψ_{pd} and Ψ_{md}, MPa) and transpiration (E_s, mmol m^{-2} s^{-1}). Plot abbreviations are *dr*, drought; *cc,* cover control; *ac*, ambient control.

Please note: Wiley-Blackwell are not responsible for the content or functionality of any supporting materials supplied by the authors. Any queries (other than missing material) should be directed to the corresponding author for the article.